Talanta 82 (2010) 377–383

Contents lists available at ScienceDirect

Talanta

journal homepage: www.elsevier.com/locate/talanta

β−cyclodextrins-based inclusion complexes of $CoFe_2O_4$ magnetic nanoparticles as catalyst for the luminol chemiluminescence system and their applications in hydrogen peroxide detection

Shaohui He[a], Wenbing Shi[a,c], Xiaodan Zhang[a], Jian Li[b], Yuming Huang[a,*]

[a] College of Chemistry and Chemical Engineering, The Key Laboratory of Luminescence and Realtime Analysis, Ministry of Education; Southwest University; Chongqing 400715, PR China
[b] College of Physical Science and Technology, Southwest University, Chongqing 400715, PR China
[c] College of Chemistry and Chemical Engineering, Yangtze Normal University, Chongqing, Fuling 408003, PR China

ARTICLE INFO

Article history:
Received 18 February 2010
Received in revised form 22 April 2010
Accepted 25 April 2010
Available online 21 May 2010

Keywords:
Inclusion complexes
$CoFe_2O_4$ magnetic nanoparticles
Chemiluminescence
Hydrogen peroxide

ABSTRACT

β−cyclodextrins (β−CD)-based inclusion complexes of $CoFe_2O_4$ magnetic nanoparticles (MNPs) were prepared and used as catalysts for chemiluminescence (CL) system using the luminol–hydrogen peroxide CL reaction as a model. The as-prepared inclusion complexes were characterized by XRD (X-ray diffraction), TGA (thermal gravimetric analysis) and FT-IR. The oxidation reaction between luminol and hydrogen peroxide in basic media initiated CL. The effect of β−CD-based inclusion complexes of $CoFe_2O_4$ magnetic nanoparticles and naked $CoFe_2O_4$ magnetic nanoparticles on the luminol–hydrogen peroxide CL system was investigated. It was found that inclusion complexes between β−CD and $CoFe_2O_4$ magnetic nanoparticles could greatly enhance the CL of the luminol–hydrogen peroxide system. Investigation on the kinetic curves and the chemiluminescence spectra of the luminol–hydrogen peroxide system demonstrates that addition of $CoFe_2O_4$ MNPs or inclusion complexes between β−CD and $CoFe_2O_4$ MNPs does not produce a new luminophor of the chemiluminescent reaction. The luminophor for the CL system was still the excited-state 3-aminophthalate anions (3-APA*). The enhanced CL signals were thus ascribed to the possible catalysis from $CoFe_2O_4$ MNPs or inclusion complexes between β−CD and $CoFe_2O_4$ nanoparticles. The feasibility of employing the proposed system for hydrogen peroxide sensing was also investigated. Experimental results showed that the CL emission intensity was linear with hydrogen peroxide concentration in the range of 1.0×10^{-7} to 4.0×10^{-6} mol L^{-1} with a detection limit of 2.0×10^{-8} mol L^{-1} under optimized conditions. The proposed method has been used to determine hydrogen peroxide in water samples successfully.

1. Introduction

Nanoparticles, which have nanostructured components (at less than 100 nm), possess unique chemical, physical, and mechanical properties [1] and have been applied in many areas (e.g., microelectronics industry, chemical sensing, biomedicine technique and environmental protection, etc.) [2,3]. Motivated by the existing and potential applications of nanomaterials, researches on nanomaterial have been expanded rapidly in the past few years. These small nanoparticles show a great potential of catalysis because of the large surface area of the particles. For example, noble metal nanoparticles are important nanomaterial for use as a reactive center [4] or as a nanocatalyst in many chemical reactions [5,6]. However, these small particles can easily aggregate in water [7]. In order to prevent this phenomenon, particles should be stabilized by a highly water-soluble protective agent. β−cyclodextrins (β−CD), a class of water-soluble cyclic oligosaccharides, have a porous shaped structure with a hydrophobic cavity and hydrophilic rims made of hydroxyl groups [8]. They have been considered to be a kind of important materials in supramolecular chemistry as molecular hosts capable of forming inclusion complexes with a large number of low molecular weight organic molecules, inorganic ions, and metallo-organic species [9–11] *via* noncovalent interactions in their hydrophobic cavities. It has been demonstrated that methylated cyclodextrins can stabilize the catalytically active noble metal nanoparticles *via* hydrophobic–hydrophobic interactions between metal nanoparticles and cyclodextrins or *via* interactions between metal nanoparticles and hydroxyl groups of native cyclodextrins in water [12] or *via* formation of host–guest inclusion complexes in water [6].

Chemiluminescent (CL) methods promise ultra sensitive detection limits (attomole–zeptomole), rapid assays, and a broad range

* Corresponding author. Tel.: +86 23 68254843; fax: +86 23 68367675.
E-mail address: yuminghuang2000@yahoo.com (Y. Huang).

0039-9140/$ – see front matter © 2010 Elsevier B.V. All rights reserved.
doi:10.1016/j.talanta.2010.04.055

of analytical applications with simple instruments (no monochromator required). However, study of CL was limited to some molecular systems [13–15]. Since the pioneer work initiated by Cui's group [16], who firstly found gold colloids with nanoparticles of different sizes could enhance the CL of the luminol–hydrogen peroxide system, the potential of nanoparticles in aqueous CL reactions has attracted widespread attention [17–19]. In fact, a careful examination of the literature indicated that most of the study focused on metallic nanoparticles (especially noble metal nanoparticles) as catalysts in aqueous media [20–27]. There are only a few reports involving the chemiluminescence of metal oxide nanoparticles in aqueous media [28–30].

In recent years, magnetic nanoparticles (MNPs) have obtained widespread attention because of their large ratio of surface area to volume, superparamagnetic behavior and low toxicity. In most investigations, magnetic nanoparticles were used as a new alternative to porous materials for supporting catalytically active agents such as a nanostructured metal catalyst [7,31–33] and ligand [34]. To the best of our knowledge, there are only a few reports involving the direct catalytic function of Fe_3O_4 magnetic nanoparticles. Gao et al. found that Fe_3O_4 MNPs were proved to possess intrinsic peroxidase-like activity similar to that found in natural peroxidases [35]. More recently, Wei and Wang have used the novel properties of Fe_3O_4 MNPs as peroxidase mimetics for a colorimetric assay of hydrogen peroxide and glucose [36].

It has been demonstrated in the study by Bocanegra-Diaz et al. [37] that the inclusion compound between magnetite and β–CD could be formed, suggesting the key role of cyclodextrins in the control of the magnetite shape and nanosize through its inclusion into the β–CD cavity. More recently, Cruz et al. [38] showed that the interaction between the magnetite and β–CD resulted in the formation of a complex with enhanced aqueous solubility. However, no study has been performed to evaluate the potential of β–CD-based inclusion complexes of magnetic nanoparticles as catalysts for chemiluminescence analysis in literature.

In the present study, β–CD-based inclusion complexes of $CoFe_2O_4$ magnetic nanoparticles, the novel classes of inclusion compounds, were chosen as catalysts for the luminol CL system. The luminol–hydrogen peroxide CL reaction was used as a model. The as-prepared inclusion complexes were characterized by XRD (X-ray diffraction), TGA (thermal gravimetric analysis) and FT-IR. The effect of β–CD-based inclusion complexes of $CoFe_2O_4$ magnetic nanoparticles and naked $CoFe_2O_4$ magnetic nanoparticles on the luminol–hydrogen peroxide CL system was investigated, and the kinetic curves and the chemiluminescence spectra of the luminol–hydrogen peroxide system in the presence of β–CD-based inclusion complexes of $CoFe_2O_4$ magnetic nanoparticles were discussed. The feasibility of employing the proposed system for hydrogen peroxide sensing was also investigated. Experimental results showed that the CL emission intensity was linear with hydrogen peroxide concentration in the range of 1.0×10^{-7}–4.0×10^{-6} mol L^{-1} with a detection limit of 2.0×10^{-8} mol L^{-1} under optimized conditions. The proposed method has been used to determine hydrogen peroxide in water samples successfully.

2. Experimental

2.1. Reagents and materials

All chemicals used in this work were of analytical grade and used as received without further purification. Luminol was from Merck (Germany), a 0.01 mol L^{-1} luminol solution was prepared by dissolving 1.772 g luminol in 1000 mL of 0.01 mol L^{-1} NaOH solutions. A hydrogen peroxide stock solution was prepared by appropriately diluting the commercial reagent (30%), its concentration was standardized by titration with $KMnO_4$. All other reagents such as sodium carbonate, sodium hydrogen carbonate, hydrochloric acid, sodium hydroxide, sodium dihydrogen phosphate, ferric chloride, and cobalt nitrate were obtained from Chongqing Chemical Reagents Company (Chongqing, China). β–CD was purchased from Shanghai Chemical Reagents Company (Shanghai, China). The $CoFe_2O_4$ MNPs was prepared according to method of Massart and co-workers [39]. All glassware was soaked in 10% nitric acid and thoroughly cleaned before use. 0.1 mol L^{-1} Na_2CO_3 solution was used as basic media for luminol CL reaction.

2.2. Preparation of the inclusion complexes

The inclusion complexes were prepared by mixing 79.4 mg L^{-1} $CoFe_2O_4$ MNPs and 1.0×10^{-4} mol L^{-1} β–CD in 25 mL 0.01 mol L^{-1} sulfuric acid, and the mixture was stirred for 20 min in room temperature, the obtained solution was kept for further use. While for characterization, the above solution was heated to dry and the resulting powder could be used for TG, XRD and FT-IR.

2.3. Instrumentation

CL measurements were performed on a MCFL-A Multifunction Chemiluminescence/Bioluminescence Analyzer (Ruike Electronic Equipment Company Ltd., Xi'an, China). The pH of the solutions were detected by a PHS-3D pH meter (Shanghai Precision Scientific Instruments Co., Ltd., China); The X-ray diffraction (XRD) patterns of the as-prepared products were measured by XD-3 X-ray diffractometer (PuXi, Beijing, China) under the conditions of nickel filtered CuKα radiation (λ = 0.15406 nm) at current of 20 mA and a voltage of 36 KV. The scanning rate was 4°/min in the angular range of 10–70° (2θ). Thermo gravimetric (TG) data was obtained by a TA-SDTQ 600 (Texas Instruments, Inc., New Castle, DE, USA) in the temperature from 25 to 500 °C at a heating rate of 10 °C/min. FT-IR spectra were recorded on a Nicolet 170SX instrument (Madison, WI, USA) in the transmission mode using KBr pellets of the sample. UV–visible spectra were recorded on a UV–2450 Shimazhu spectrophotometer (Shuzhou, China). The CL spectra were recorded on an F-4500 spectrofluorimeter (Hitachi, Japan) under the model of fluorescence scan by turning off the excitation light.

2.4. General procedure for CL analysis

A schematic diagram of flow system used in this work is shown in Fig. 1. Two peristaltic pumps were used to deliver all solutions; one at a flow rate of 3 mL/min (per tube) for delivering the catalyst solution ($CoFe_2O_4$ or β–CD-$CoFe_2O_4$ inclusion complexes) and water carrier stream; the other for delivering CL reaction reagents (luminol and hydrogen peroxide) at a flow rate of 3 mL/min (per tube). PTFE tubing (0.8 mm i.d.) was used to connect all components in the flow system. For CL measurement, flow lines were inserted into the luminol solution, hydrogen peroxide solution, water, and $CoFe_2O_4$ or inclusion complexes solution, respectively. Then the pumps were started until a stable baseline was recorded. Injection was made by using an eight-way injection valve equipped with a 200 μL sample loop. The CL signal produced in the flow cell was detected by a photomultiplier tube (operated at −500 V) of the Type MCFL-A Multifunction Chemiluminescence/Bioluminescence Analyzer. The signal was recorded by a computer, equipped with a data acquisition interface. Data acquisition and treatment were performed with REMAX software running under Windows XP. For characterization of the chemiluminescent analysis system, aqueous standards were used. A series of working standard solution with different concentrations were prepared by diluting a concentrated fresh standard solution of hydrogen peroxide with water. The net

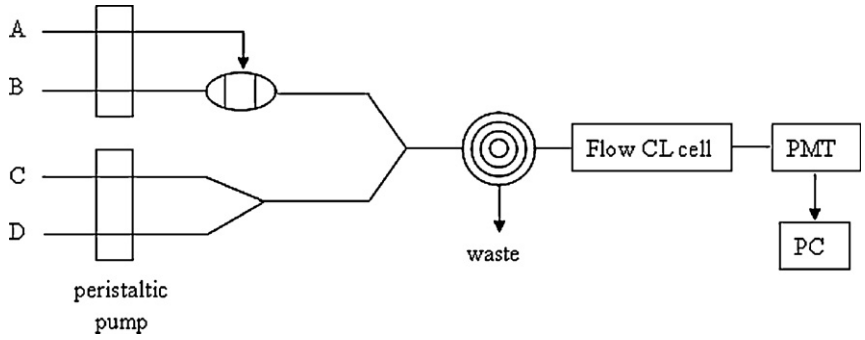

Fig. 1. Schematic diagram of the FIA-CL flow system. A: $CoFe_2O_4$ MNPs or the inclusion complexes, B: H_2O, C: luminol, D: hydrogen peroxide, PMT: photomultiplier tube, PC: personal computer.

CL emission intensity ($\Delta I = I_1 - I_0$, where I_1 is the CL intensity of sample solution, I_0 the blank solution) *versus* hydrogen peroxide concentration was used for the calibration. At each hydrogen peroxide concentration, the injection was repeated for at least three times, and the average CL signal was obtained. Catalytic properties can be evaluated by CL emission intensities *versus* concentrations of hydrogen peroxide.

2.5. Procedure for water samples

One tap water sample and two river water samples were collected from laboratory and Jialing River, Changjiang River, respectively. For real water sample analysis, EDTA as masking agent was added to environmental water samples with final concentration of 1.0×10^{-6} mol L^{-1} for eliminating the potential interference of metal ions.

3. Results and discussion

The aim of the present study was to investigate the β–CD-based inclusion complexes of magnetic nanoparticles, the novel classes of inclusion compounds, as catalysts for the luminol CL system. To study this, the comparison experiments using different magnetic nanoparticle materials such as γ-Fe_2O_3, Fe_3O_4, and $CoFe_2O_4$ were performed using the luminol–hydrogen peroxide CL reaction as a model. And the experimental results were shown in Fig. 2. As can be seen that $CoFe_2O_4$ magnetic nanoparticles show higher catalytic activity as compared with the other magnetic nanoparticles. So, we choose $CoFe_2O_4$ magnetic nanoparticles for further study in the present work.

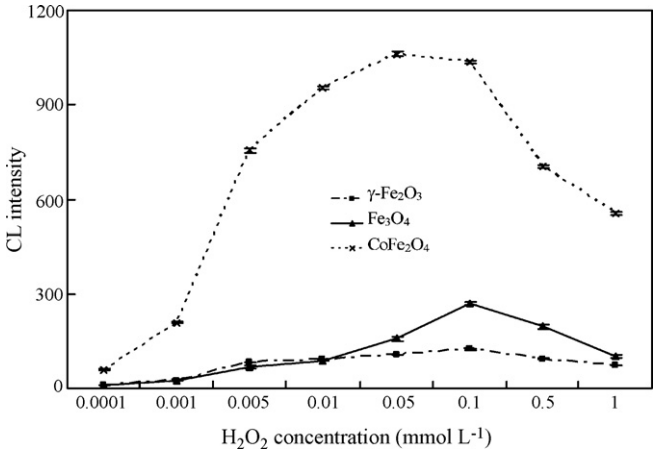

Fig. 2. Comparison of catalytical activities using different magnetic nanoparticles as catalyst. Luminol concentration: 1.0×10^{-6} mol L^{-1} in 0.1 mol L^{-1} Na_2CO_3(pH 11.2); Concentration of magnetic nanoparticles: 1 mg L^{-1}. Error bars represent one standard deviation for three measurements.

3.1. Characterization of the inclusion complexes between β–CD and $CoFe_2O_4$ MNPs

Fig. S1 (Supplementary information) presents the typical TG curves of the original β–CD, $CoFe_2O_4$ MNPs, and the inclusion complexes between β–CD and $CoFe_2O_4$ MNPs. The weight-loss stage below 300 °C is a result of the evaporation of physically adsorbed water in the sample. The pure β–CD is decomposed completely from 300 °C through 350 °C, the inclusion complexes have less decomposition than the pure β–CD. For example, the TG curve for the inclusion complexes featured an early decomposition of the host to be about 230 °C, which was attributed to the promoting effects of the $CoFe_2O_4$ MNPs on the decomposition of the β–CD, and was an evidence of a significant strong host–guest affinity [40]. While the $CoFe_2O_4$ MNPs do not show any degradation. This confirms the formation of the host–guest complexes between $CoFe_2O_4$ MNPs and β–CD.

XRD is a widely used technique in the study of inclusion complexes for assessing the structure and to check whether a new compound has been produced from the parent molecules [41]. Fig. S2 (Supplementary information) shows the XRD patterns of β–CD, $CoFe_2O_4$ MNPs, and the inclusion complexes. Sharp peaks over the diffraction angles indicate the crystal nature of β–CD (Fig. S2a) and $CoFe_2O_4$ MNPs (Fig. S2b). In contrast, the diffraction diagrams of the inclusion complexes (Fig. S2c) exhibit a dramatic decrease in the number and intensity of diffraction peaks, suggesting formation of a new amorphous inclusion complexes.

The FT-IR spectra of β–CD (Fig. S3a) and the inclusion complexes (Fig. S3b) in the region from 400 to 4000 cm^{-1} are presented in Fig. S3. As can be seen that the positions and relative intensities of a few bands for both the host and the guest are affected by the formation of the inclusion complexes [42]. For example, the absorption bands at 3408, 2928 cm^{-1} attributed to O–H stretching mode and C–H stretching mode of β–CD shifted to a more broaden band at 3441 cm^{-1} in inclusion complexes. The positions and relative intensities changed in the inclusion complexes for the bands at 1404 cm^{-1} assigned to C–H bending mode of β–CD and at 1157, 1083, 1029 cm^{-1} mainly corresponding to the stretch vibrations of C–H, C–C, C–O and C–O–C of glucose units of β–CD. In addition, the bands at 757 cm^{-1} due to ring breathing vibration, 707 and 578 cm^{-1} due to pyranose ring vibration of β–CD decreased sharply in the inclusion complexes, which could be interpreted as the 'fixed' nature of the β–CD that prevented the pyranose ring vibration [43].

3.2. The characteristics of luminol CL in the presence of the inclusion complexes between β–CD and $CoFe_2O_4$ MNPs

Fig. 3 shows the kinetic curves of the luminol CL system in the presence of β–CD, $CoFe_2O_4$ MNPs, and the inclusion complexes

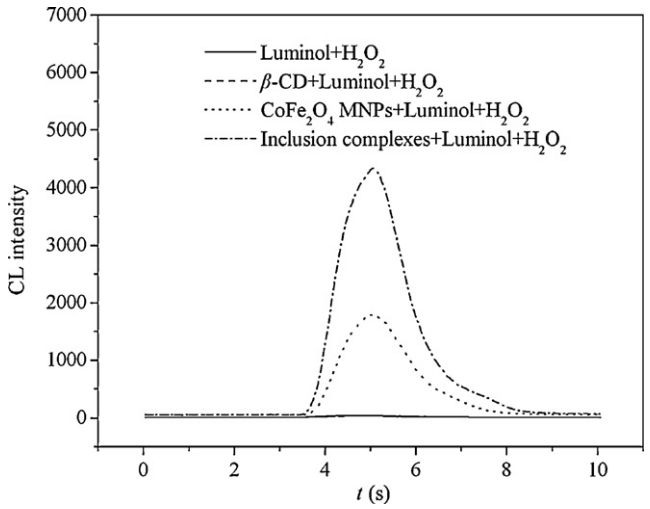

Fig. 3. Kinetic characteristics of the luminol–hydrogen peroxide–inclusion complexes between β–CD and $CoFe_2O_4$ MNPs CL system. Luminol concentration: 1.0×10^{-6} mol L^{-1} in 0.1 mol L^{-1} Na_2CO_3(pH 11.2); hydrogen peroxide concentration: 1.0×10^{-6} mol L^{-1}; β–CD concentration: 5.0×10^{-5} mol L^{-1}; $CoFe_2O_4$ concentration: 39.7 mg L^{-1}; Inclusion complexes were made by 39.7 mg L^{-1} $CoFe_2O_4$ and 5.0×10^{-5} mol L^{-1} β–CD.

between β–CD and $CoFe_2O_4$ MNPs. As can be seen that no significant enhancement effects were found for β–CD. However, $CoFe_2O_4$ MNPs, and the inclusion complexes between β–CD and $CoFe_2O_4$ MNPs showed the enhancement effects of luminol CL, in which the most intensed CL signal occurred for the β–CD-based inclusion complexes of $CoFe_2O_4$ MNPs. In order to study the role of $CoFe_2O_4$ MNPs and the inclusion complexes between β–CD and $CoFe_2O_4$ MNPs, the chemiluminescence spectra of following systems were studied by the F-4500 fluorimetry: (a) luminol/hydrogen peroxide; (b) β–CD/luminol/hydrogen peroxide; (c) $CoFe_2O_4$ MNPs/luminol; (d) $CoFe_2O_4$ MNPs/luminol/hydrogen peroxide; (e) inclusion complexes/luminol/hydrogen peroxide. The results shown in Fig. 4

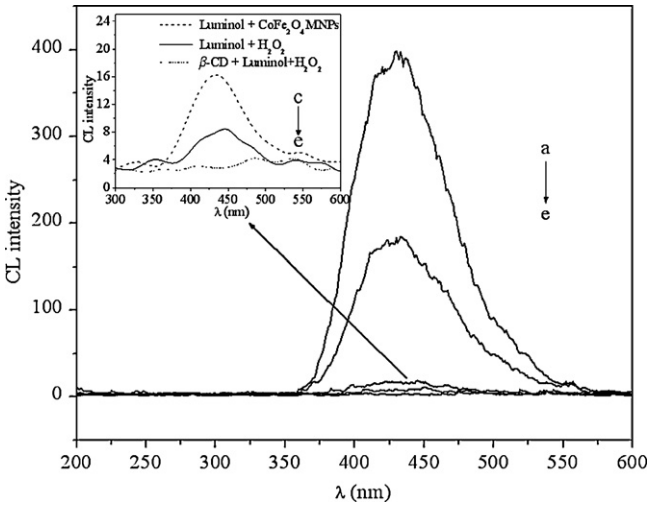

Fig. 4. CL spectra for the luminol–hydrogen peroxide–inclusion complexes between β–CD and $CoFe_2O_4$ system. (a): Inclusion complexes + luminol + hydrogen peroxide; (b): $CoFe_2O_4$ + luminol + hydrogen peroxide; (c): $CoFe_2O_4$ + luminol; (d): luminol + hydrogen peroxide; (e): β–CD + luminol + hydrogen peroxide; Luminol concentration: 1.0×10^{-4} mol L^{-1} in 0.1 mol L^{-1} Na_2CO_3(pH 11.2); hydrogen peroxide concentration: 1.0×10^{-5} mol L^{-1}; β–CD concentration: 1.0×10^{-5} mol L^{-1}; $CoFe_2O_4$ concentration: 8.0 mg L^{-1}; Inclusion complexes were made by 8.0 mg L^{-1} $CoFe_2O_4$ and 1.0×10^{-5} mol L^{-1} β–CD. Inset: Amplified CL spectra for (c): $CoFe_2O_4$ + luminol, (d): luminol + hydrogen peroxide, and (e): β–CD + luminol + hydrogen peroxide, respectively.

demonstrate that all the above systems give one peak situating at about 425 nm (same as the maximum emission spectra of 3-aminophthalate), indicating that the role of $CoFe_2O_4$ MNPs or inclusion complexes between β–CD and $CoFe_2O_4$ MNPs is only an enhancement reagent because there is no new emitter produced in the reaction. Therefore, it can be concluded that addition of $CoFe_2O_4$ MNPs or inclusion complexes between β–CD and $CoFe_2O_4$ MNPs does not produce a new luminophor of the chemiluminescent reaction. The luminophor for the CL system was still the excited-state 3-aminophthalate anions (3-APA*). The enhanced CL signals were thus ascribed to the possible catalysis from $CoFe_2O_4$ MNPs or inclusion complexes between β–CD and $CoFe_2O_4$ nanoparticles. Due to its highest CL enhancement effect on the luminol–hydrogen peroxide system, the β–CD-based inclusion complexes of $CoFe_2O_4$ MNPs were selected for further study.

3.3. Optimization of chemiluminescence reaction

The experimental conditions were optimized for the luminol–hydrogen peroxide CL system in the presence of inclusion complexes between β–CD and $CoFe_2O_4$ MNPs as shown in Fig. 5. The effect of pH on CL was studied in the range of pH 8.5–12.5 (0.1 mol L^{-1} sodium carbonate). As can be seen (Fig. 5A), when the pH of the luminol solution was lower than pH 11.2, the CL intensity increased with increasing pH. When the pH of the luminol solution was higher than pH 11.2, the CL intensity decreased with increasing pH. The optimized pH condition for the studied CL system was pH 11.2. The effect of luminol concentration on CL was studied in the range from 1.0×10^{-8} to 1.0×10^{-5} mol L^{-1}. The result is shown in Fig. 5B. The CL intensity increased with increasing luminol concentration in the range of 1.0×10^{-8} to 1.0×10^{-5} mol L^{-1}. Sharp increase in CL signal intensity was observed when the concentration of luminol was lower than 0.5×10^{-6} mol L^{-1}. However, only slight changes in light intensity were observed when the concentration of luminol was above 5.0×10^{-6} mol L^{-1}. Considering the background level, finally, 1.0×10^{-6} mol L^{-1} was chosen as the optimal lumimol concentration in the present study. The effects of the concentration of the inclusion complexes (as $CoFe_2O_4$) in the range of 0.8–79.4 mg L^{-1} were also investigated, as shown in Fig. 5C. The CL intensity increased with increasing concentration of the inclusion complexes up to 39.7 mg L^{-1}, above which, the CL intensity decreased. So, 39.7 mg L^{-1} of the inclusion complexes was selected. The effect of hydrogen peroxide concentration was investigated ranging from 1.0×10^{-7} to 2.0×10^{-5} mol L^{-1} (Fig. 5D). The experimental results showed that the CL intensity increased with increasing concentration of hydrogen peroxide concentration up to 1.0×10^{-5} mol L^{-1}, above which, the CL intensity decreased. In summary, the optimized conditions for the luminol–hydrogen peroxide–inclusion complexes between β–CD and $CoFe_2O_4$ MNPs CL system are as follows: 1.0×10^{-6} mol L^{-1} lumimol in 0.1 mol L^{-1} sodium carbonate, 1.0×10^{-5} mol L^{-1} hydrogen peroxide, and 39.7 mg L^{-1} (as $CoFe_2O_4$) of inclusion complexes between β–CD and $CoFe_2O_4$ MNPs.

3.4. Analytical performance

The possibility of using the proposed method for the determination of hydrogen peroxide was investigated. The calibration graphs for the determination of hydrogen peroxide were constructed under the optimum conditions described above. The calibration graph of emission intensity *versus* hydrogen peroxide concentration was linear in the 1.0×10^{-7} to 4.0×10^{-6} mol L^{-1} range. The regression equation is $\Delta I = 11 + 1351$[hydrogen peroxide] (μmol L^{-1}), $r^2 = 0.9989$ ($n = 8$). The limit of detection (LOD, 3σ) for hydrogen peroxide was 2.0×10^{-8} mol L^{-1}. The RSD was

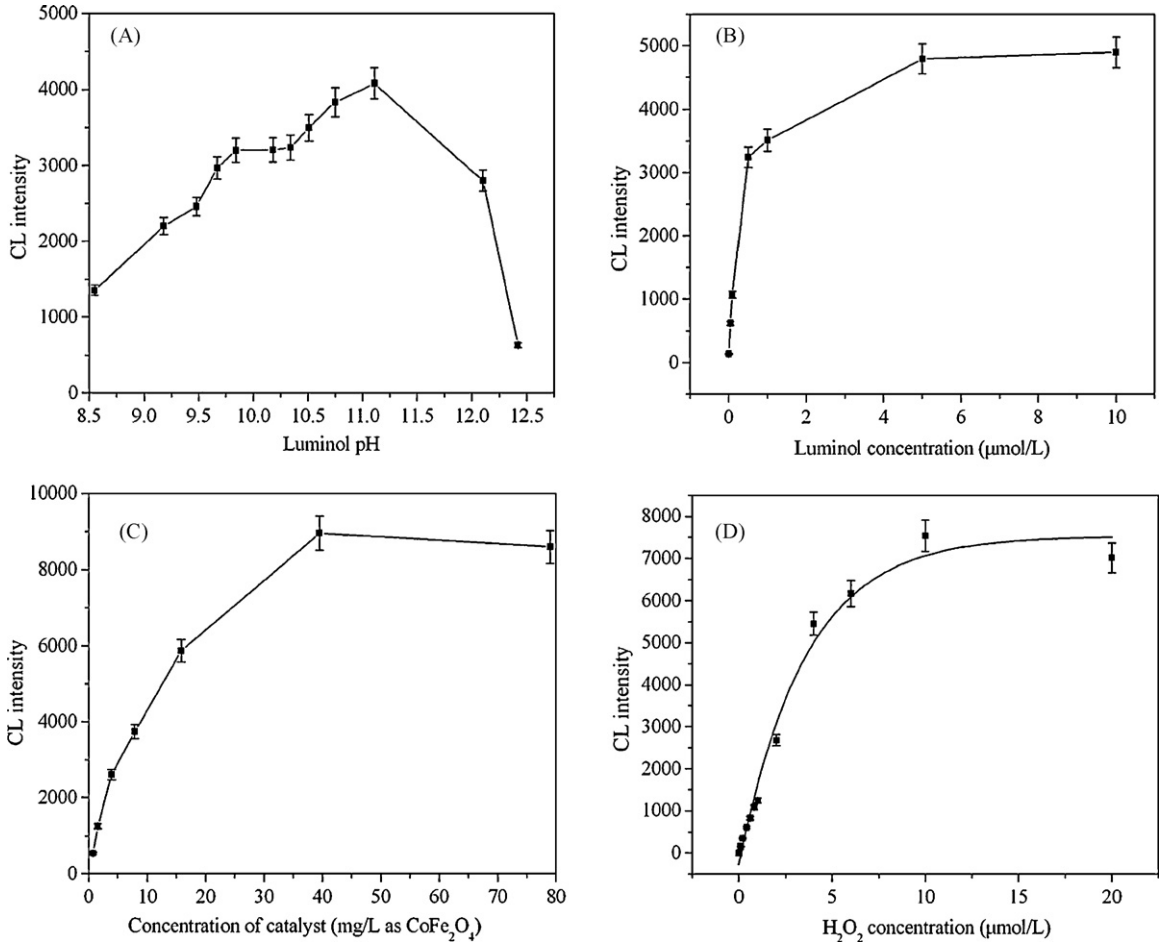

Fig. 5. Effects of the reactant conditions on the luminol–hydrogen peroxide CL system in the presence of inclusion complexes between β–CD and $CoFe_2O_4$ MNPs. (A) Effect of pH of luminol: 1.0×10^{-6} mol L^{-1} luminol, 1.0×10^{-6} mol L^{-1} hydrogen peroxide, 8.0 mg L^{-1} (as $CoFe_2O_4$) inclusion complexes. (B) Effect of luminol concentration: 0.1 mol L^{-1} Na_2CO_3 (pH 11.2), 1.0×10^{-6} mol L^{-1} hydrogen peroxide, 8.0 mg L^{-1} (as $CoFe_2O_4$) inclusion complexes. (C) Effect of catalyst concentration: 1.0×10^{-6} mol L^{-1} luminol (pH 11.2), 1.0×10^{-6} mol L^{-1} hydrogen peroxide, 8.0 mg L^{-1} inclusion complexes (as $CoFe_2O_4$). (D) Effect of hydrogen peroxide concentration: 1.0×10^{-6} mol L^{-1} luminol in 0.1 mol L^{-1} sodium carbonate (pH 11.2), 39.7 mg L^{-1} (as $CoFe_2O_4$) inclusion complexes. Error bars represent one standard deviation for three measurements.

3.4% for 5.0×10^{-7} mol L^{-1} hydrogen peroxide ($n = 11$). The present method was compared to the analytical methods previously published in literatures [29,44–50] using luminol–H_2O_2 CL system with and without nanoparticles for H_2O_2 analysis in terms of LODs (the detection limits). And the LODs were listed in Table 1. As can be seen, the LOD of this work was at least one order of magnitude lower than the reported other luminol–H_2O_2 CL methods [29,44,45,47–49], showing high sensitivity of the proposed method for H_2O_2 analysis. Also, the LOD of this method was comparable with that obtained by Au nanoparticles or QDs-based electrochemiluminescence methods [50,51].

3.5. *Effect of foreign substances*

The effect of foreign substances was tested by analyzing a standard solution of hydrogen peroxide (1.0×10^{-6} mol L^{-1}) to which increasing amounts of foreign substances was added. The tolerable concentration ratios with respect to 1.0×10^{-6} mol L^{-1} hydrogen peroxide for interference at less than 10% level were listed in Table 2. In order to examine the water constituents on hydrogen peroxide determination, the chemical components in the water samples investigated in the present study were conducted and the concentrations level (mg L^{-1}) are as fol-

Table 1
Comparison LOD of this work with some established methods using chemiluminescence for hydrogen peroxide.

System	Detection limit (μmol L^{-1})	Analytical method	Reference
Hexacyanoferrate(III)–luminol–H_2O_2	1.8	CL	[44]
Immobilized Co^{2+} and sodium lauryl sulfate–luminol–H_2O_2	0.26	CL sensor	[45]
KIO_4–luminol–H_2O_2	0.03	CL	[46]
Immobilized HRP–luminol–H_2O_2	670	CL sensor	[47]
Ferric oxide nanoparticles–luminol–H_2O_2	1250	CL	[29]
Au nanoparticles–Hb/PMMA–luminol–H_2O_2	0.2	CL imaging	[48]
Au nanoflower–luminol–H_2O_2	10	CL	[49]
Au nanoparticles–luminol–H_2O_2	0.1	ECL	[50]
Thiol capped CdTe QDs–H_2O_2	0.06	ECL	[51]
β–CD/$CoFe_2O_4$ MNPs/luminol/H_2O_2	0.02	CL	This work

Table 2
Recoveries of hydrogen peroxide in the presence of foreign species (hydrogen peroxide concentration: 1.0×10^{-6} mol L^{-1}).

Coexisting species	At concentration	Recovery (%)[a]	Coexisting species	At concentration	Recovery (%)[a]
Na^+	23 mg L^{-1}	95.99 ± 0.95	Cu^{2+}	65 μg L^{-1}	97.44 ± 1.38
K^+	39 mg L^{-1}	101.00 ± 0.47	Cu^{2+}-EDTA[b]	130 μg L^{-1}	97.92 ± 2.57
NH_4^+	9 mg L^{-1}	110.00 ± 1.08	Fe^{3+}	56 μg L^{-1}	118.29 ± 0.46
Ca^{2+}	20 mg L^{-1}	102.17 ± 3.65	Fe^{3+}-EDTA[b]	280 μg L^{-1}	99.32 ± 1.22
Mg^{2+}	7 mg L^{-1}	99.80 ± 0.11	Cl^-	36 mg L^{-1}	101.00 ± 0.47
Zn^{2+}	6.5 mg L^{-1}	101.84 ± 0.59	NO_3^-	62 mg L^{-1}	95.99 ± 0.95
Pb^{2+}	4 mg L^{-1}	96.93 ± 0.36	SO_4^{2-}	49 mg L^{-1}	91.46 ± 0.84
Al^{3+}	0.14 mg L^{-1}	99.14 ± 3.28	$H_2PO_4^-$	45 mg L^{-1}	98.65 ± 1.41
Ni^{2+}	300 μg L^{-1}	95.60 ± 1.54	HPO_4^{2-}	19 mg L^{-1}	99.12 ± 1.59
Cr^{3+}	50 μg L^{-1}	100.66 ± 4.28	I^-	1200 μg L^{-1}	102.96 ± 1.88
Co^{2+}	60 μg L^{-1}	105.06 ± 1.63			

[a] Mean value ± standard deviation ($n = 3$).
[b] EDTA concentration: 1.0×10^{-6} mol L^{-1}.

lows: K: 1.8–2.2, Na: 10.8–18.3, Ca: 15.2–20.3, Mg: 5.1–5.5, Al: 0.15–0.18, Cu(II):0.045–0.048, Zn(II): nd (not detected)–0.01, Pb(II): 0.13–0.17, Mn(II): nd (not detected), Cd(II): 0.009–0.013, Fe: 0.018–0.037, Cr(III): 0.001–0.016, NH_4^+: nd (not detected)–1.6, sulfate: 29.8–42.8, phosphate: <0.5, chloride: 13.4–17.1, iodide and fluoride: nd (not detected), nitrate: 2.6–7.2. As can be seen that Fe, Al are the main interferences for hydrogen peroxide determination. In order to eliminate the interferences derived from Fe, Al and other coexisting transient metals, EDTA was selected as chelate reagent for the present study. Experimental results indicate that addition of EDTA could realize quantitative recovery of hydrogen peroxide from water samples as compared to those without EDTA addition. Hence, for real sample analysis for hydrogen peroxide, EDTA was selected.

3.6. Determination of hydrogen peroxide in water samples

The proposed method was applied to hydrogen peroxide determination in environmental water samples. In order to eliminate the possible interferences from metal ions, EDTA was used as masking reagent. As can be seen from Table 3 that the recoveries of hydrogen peroxide in the spiked environmental water samples ranged from 81% to 104%, which demonstrated that the proposed method was satisfactory for hydrogen peroxide analysis.

Table 3
Results of the determination of hydrogen peroxide in water samples.

Sample	Found (10^{-6} mol L^{-1})	Added (10^{-6} mol L^{-1})	Total found (10^{-6} mol L^{-1})	Recovery (%)
Jialing river	nd[a]	1.0	0.81	81.3
Changjiang river	0.08	1.0	0.99	97.8
Tap water	0.02	1.0	1.06	104.5

[a] nd: not detected.

3.7. Possible CL mechanism

It is well known that luminol can react with hydrogen peroxide to produce weak CL in alkaline conditions [52]. And the superoxide anion ($O_2^{\bullet -}$) or hydroxyl radical ($OH^{\bullet}$) as the impor-

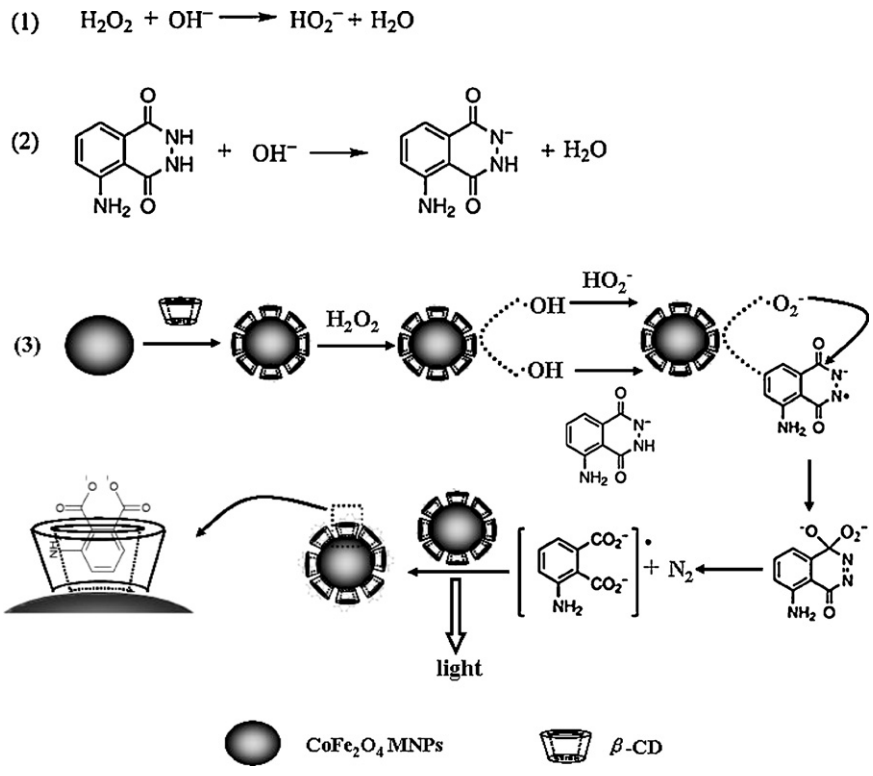

Scheme 1. Possible CL process of luminol–H_2O_2 in the presence of inclusion complexes between β–CD and $CoFe_2O_4$ MNPs.

tant intermediates was supposed to be involved in the reaction [53,54]. When adding $CoFe_2O_4$ MNPs in the luminol–hydrogen peroxide system, $CoFe_2O_4$ MNPs may interact with the reactants or the intermediates of the reaction of luminol with hydrogen peroxide. It is possible that $CoFe_2O_4$ MNPs as the catalysts could catalyze the decomposition of H_2O_2 to yield active intermediates such as $OH^{\bullet}$ and $O_2^{\bullet -}$. The hydroxyl radical reacted with luminol to form luminol radical ($L^{\bullet -}$), then the produced $L^{\bullet -}$ reacts with superoxide anion, yielding an unstable endoperoxide and an electronically excited 3-aminophthalate anion (3-APA*), leading to light emission. As a result, the emission was enhanced. On the other hand, it has been demonstrated that β–CD can stabilize the catalytically active nanoparticles *via* hydrophobic–hydrophobic interactions between metal nanoparticles and cyclodextrins or *via* interactions between metal nanoparticles and hydroxyl groups of native cyclodextrins in water [12]. In our case, it is assumed that β–CD on the surface of $CoFe_2O_4$ MNPs can stabilize $CoFe_2O_4$ MNPs *via* formation of inclusion compound. According to Maeztu et al., the stabilization of the CL intermediate 3-APA* by β–CD could enhance the CL emission [55]. So, the β–CD-based inclusion complexes of $CoFe_2O_4$ MNPs showed higher CL response as compared with the naked $CoFe_2O_4$ MNPs due to the formation of inclusion compound between $CoFe_2O_4$ MNPs and β–CD. Based on above discussion, the possible CL enhancement processes of the present CL reaction catalyzed by β–CD-based inclusion complexes of $CoFe_2O_4$ MNPs could be expressed in a simple form as shown in Scheme 1.

4. Conclusion

In summary, we propose a novel class of inclusion compounds, namely, β–CD-based inclusion complexes of $CoFe_2O_4$ magnetic nanoparticles as catalysts for the CL system using luminol–hydrogen peroxide CL reaction as a model in this study. Investigation on the kinetic curves and the chemiluminescence spectra of the luminol–hydrogen peroxide system demonstrates that addition of $CoFe_2O_4$ MNPs or inclusion complexes between β–CD and $CoFe_2O_4$ MNPs does not produce a new luminophor of the chemiluminescent reaction. The luminophor for the CL system was still the excited-state 3-aminophthalate anions (3-APA*). The current investigation has demonstrated well the potential of inclusion complexes based on β–CD and nanoparticles as an efficient enhancement reagent for the luminol CL system. The proposed method promises high sensitivity and good reproducibility for hydrogen peroxide determination and has been used to determine hydrogen peroxide in water samples successfully.

Acknowledgment

The financial support of the research by the Natural Science Foundation of Chongqing (No. 2009BB8101) is gratefully acknowledged.

Appendix A. Supplementary data

Supplementary data associated with this article can be found, in the online version, at doi:10.1016/j.talanta.2010.04.055.

References

[1] C. Burda, X.B. Chen, R. Narayanan, M.A. El-Sayed, Chem. Rev. 105 (2005) 1025.
[2] M.S. Mauter, M. Elimelech, Environ. Sci. Technol. 42 (2008) 5843.
[3] N.L. Rosi, C.A. Mirkin, Chem. Rev. 105 (2005) 1547.
[4] A.C. Templeton, W.P. Wuelfing, R.W. Murray, Acc. Chem. Res. 33 (2000) 27.
[5] V. Méevellec, B. Leger, M. Mauduit, A. Roucoux, Chem. Commun. (2005) 2838.
[6] C. Hubert, A. Denicourt-Nowicki, A. Roucoux, D. Landy, B. Leger, G. Crowyn, E. Monflier, Chem. Commun. (2009) 1228.
[7] H.H. Yang, S.Q. Zhang, X.L. Chen, Z.X. Zhuang, J.G. Xu, X.R. Wang, Anal. Chem. 76 (2004) 1316.
[8] Y. Hou, H. Kondoh, M. Shimojo, E.O. Sako, N. Ozaki, T. Kogure, T. Ohta, J. Phys. Chem. B 109 (2005) 4845.
[9] S. Zhou, L. Wang, A. Zhang, K. Lin, W. Liu, J. Agric. Food Chem. 56 (2008) 2708.
[10] Y. Gao, X. Zhao, B. Dong, L. Zheng, N. Li, S. Zhang, J. Phys. Chem. B 110 (2006) 8576.
[11] J.A. Fernandes, S. Lima, S.S. Braga, M. Pillinger, P. Ribeiro-Claro, J.E. Rodriguez-Borges, A.D. Lopes, J.J.C. Teixeira-Dias, I.S. Goncüalves, Organometallics 24 (2005) 5673.
[12] A. Nowicki, Y. Zhang, B. Léger, J.P. Rolland, H. Bricout, E. Monflier, A. Roucoux, Chem. Commun. (2006) 296.
[13] J.L. Adcock, P.S. Francis, N.W. Barnett, Anal. Chim. Acta 601 (2007) 36.
[14] B.A. Gorman, P.S. Francis, N.W. Barnett, Analyst 131 (2006) 616.
[15] C.A. Marquette, L.J. Blum, Anal. Bioanal. Chem. 385 (2006) 546.
[16] Z.F. Zhang, H. Cui, C.Z. Lai, L.J. Liu, Anal. Chem. 77 (2005) 3324.
[17] B.A. Gorman, P.S. Francis, D.E. Dunstan, N.W. Barnett, Chem. Commun. 4 (2007) 395.
[18] J.M. Lin, M.L. Liu, J. Phys. Chem. B 112 (2008) 7850.
[19] C.F. Duan, H. Cui, Chem. Commun. (2009) 2574.
[20] H. Cui, Z.F. Zhang, M.J. Shi, J. Phys. Chem. B 109 (2005) 3099.
[21] J.Z. Guo, H. Cui, J. Phys. Chem. C 111 (2007) 12254.
[22] L. Wang, P. Yang, Y.X. Li, H.Q. Chen, M.G. Li, F.B. Luo, Talanta 72 (2007) 1066.
[23] S.F. Li, X.Z. Li, J. Xu, X.W. Wei, Talanta 75 (2008) 32.
[24] A. Safavi, G. Absalan, F. Bamdad, Anal. Chim. Acta 610 (2008) 243.
[25] S.F. Li, X.M. Zhang, Z.J. Yao, R. Yu, F. Huang, X.W. Wei, J. Phys. Chem. C 113 (2009) 15586.
[26] E.G. Zisimopoulos, G.Z. Tsogas, D.L. Giokas, N.I. Kapakoglou, A.G. Vlessidis, Talanta 79 (2009) 893.
[27] X.L. Chen, J. Yang, S.J. Xu, L.J. Xiao, Chin. J. Anal. Chem. 37 (2009) 1662.
[28] S.F. Li, X.M. Zhang, W.X. Du, Y.H. Ni, X.W. Wei, J. Phys. Chem. C 113 (2009) 1046.
[29] T.M. Triantis, K. Papadopoulos, E. Yannakopouloua, D. Dimotikali, J. Hrbáč, R. Zbořil, Chem. Eng. J. 144 (2008) 483.
[30] K.H. Liu, L.S. Yan, G.A. Luo, Chin. J. Anal. Chem. 33 (2005) 847.
[31] F. Shi, M.K. Tse, S. Zhou, M.M. Pohl, J. Radnik, S. Hübner, K. Jähnisch, A. Brückner, M. Beller, J. Am. Chem. Soc. 131 (2009) 1775.
[32] H. Ebrand, K. Mackenzie, F.D. Kopinke, Environ. Sci. Technol. 43 (2009) 3254.
[33] R. Abu-Rezig, H. Alper, D. Wang, M.L. Post, J. Am. Chem. Soc. 128 (2006) 5279.
[34] G. Chouhan, D. Wang, H. Alper, Chem. Commun. (2007) 4809.
[35] L. Gao, J. Zhuang, L. Nie, J. Zhang, Y. Zhang, N. Gu, T. Wang, J. Feng, D. Yang, S. Perrett, X. Yan, Nat. Nanotechnol. 2 (2007) 577.
[36] H. Wei, E. Wang, Anal. Chem. 80 (2008) 2250.
[37] A. Bocanegra-Diaz, N.D.S. Mohallem, R.D. Sinisterra, J. Braz. Chem. Soc. 14 (2003) 936.
[38] L.A.C. Cruz, C.A.M. Perez, H.A.M. Romero, P.E.G. Casillas, J. Alloys Compd. 466 (2008) 330.
[39] F.A. Tourinho, R. Franck, R. Massart, J. Mater. Sci. 25 (1990) 3249.
[40] A. Harada, K. Saeki, S. Takahashi, Organometallics 8 (1989) 730.
[41] P. Lo Nostro, I. Santoni, M. Bonini, P. Baglioni, Langmuir 19 (2003) 2313.
[42] C.C. Rusa, C. Luca, A.E. Tonelli, Macromolecules 34 (2001) 1318.
[43] Y.J. Huang, D. Li, J.H. Li, Chem. Phys. Lett. 389 (2004) 14.
[44] O.D. Leite, O. Fatibello, H.J. Vieira, F.R.P. Rocha, N.M. Cury., Anal. Lett. 40 (2007) 3148.
[45] A. Tahirovic, A. Copra, E. Omanovic-Miklicanin, K. Kalcher, Talanta 72 (2007) 1378.
[46] Y. Zhou, T. Nagaoka, F. Li, G. Zhu, Talanta 48 (1999) 461.
[47] A. Navas Díaz, M.C. Ramos Peinado, M.C. Torijas Minguez, Anal. Chim. Acta 363 (1998) 221.
[48] L.R. Luo, Z.J. Zhang, L.Y. Zhou, Anal. Chim. Acta 584 (2007) 106.
[49] H. Cui, W. Wang, J. Phys. Chem. C 112 (2008) 10759.
[50] H. Cui, W. Wng, C.F. Duan, G.Z. Guo, Y.P. Dong, Chem.-Eur. J. 13 (2007) 6975.
[51] H.Y. Han, Z.G. Sheng, J.G. Liang, Anal. Chim. Acta 596 (2007) 73.
[52] D.-Q. Yuan, J. Lu, M. Atsumi, J.-M. Yan, M. Kai, K. Fujita, Org. Biomol. Chem. 5 (2007) 2932.
[53] G. Merenyi, J. Lind, T.E. Eriksen, J. Biolumin. Chemilumin. 5 (1990) 53.
[54] K. Faulkner, I. Fridovich, J. Free Radic. Biol. Med. 15 (1993) 447.
[55] R. Maeztu, G. Tardajos, G. González-Gaitano, J. Phys. Chem. B 114 (2010) 2798.